Kotak et al., http://www.jcb.org/cgi/content/full/jcb.201203166/DC1

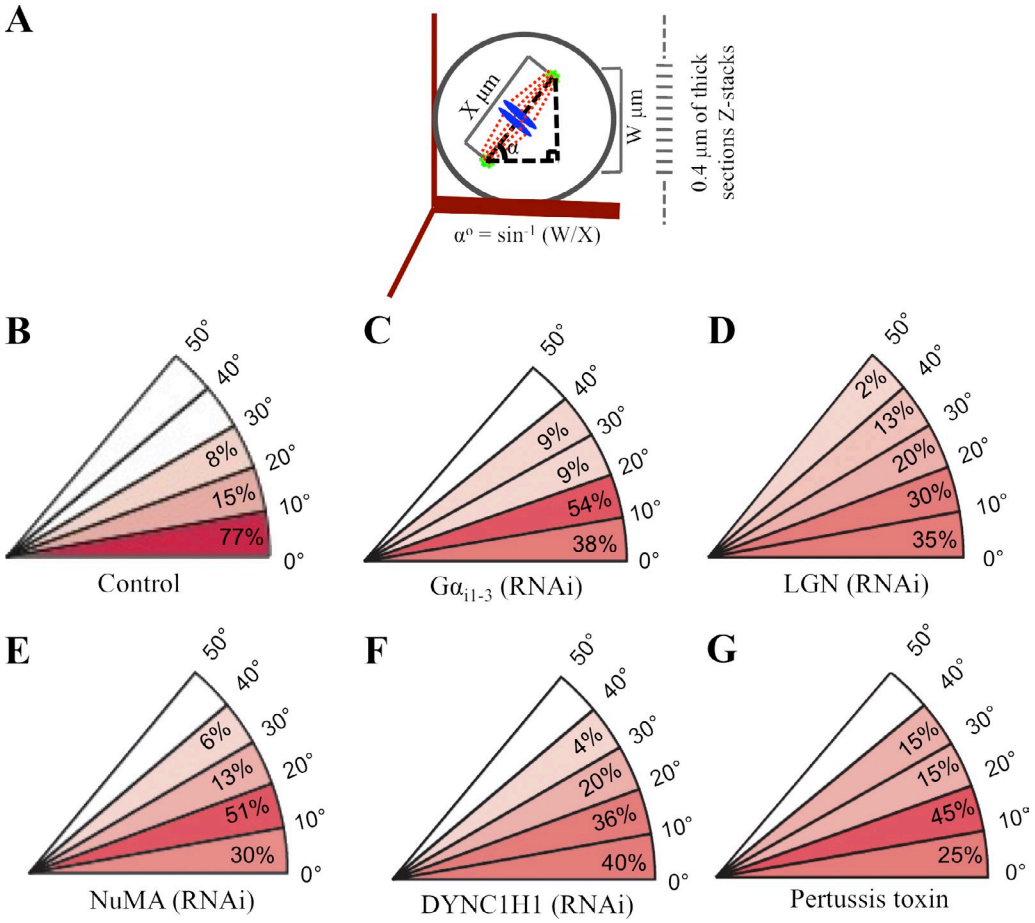

Figure S1. **Ternary complex (Gαi–LGN–NuMA) components and dynein are required for spindle positioning in HeLa cells.** (A) Analysis of metaphase spindle positioning performed by computing the distance (X; in micrometers) between the two spindle poles. The angle was calculated by imaging z stacks of 0.4-µm-thick sections and calculating the angle using an inverse trigonometric function, as illustrated. (B–G) Distribution of metaphase spindle angles with respect to the fibronectin substratum upon siRNA-mediated depletion of $G\alpha i_{1-3}$ (C), LGN (D), NuMA (E), or DYNC1H1 (F) as well as upon treatment with Pertussis toxin (G). 50 cells were analyzed for each condition, the results were rounded up to the nearest integer, and the significance was compared with control cells (two-tailed Student's *t* test; in all cases, $P < 0.005$ in comparison with control scrambled siRNAs).

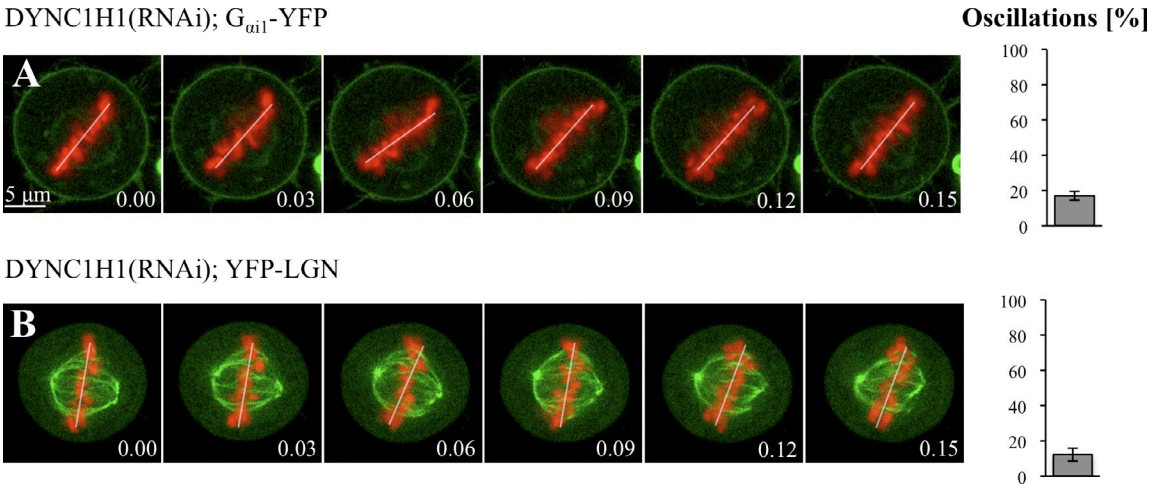

Figure S2. **Dynein function is necessary for ternary complex–induced spindle oscillations in HeLa cells.** (A and B) Images from time-lapse microscopy of metaphase HeLa Kyoto cells stably expressing GFP–α-tubulin as well as mCherry-H2B and transfected with $G\alpha i_1$-YFP and DYNC1H1 siRNAs (A) or YFP-LGN and DYNC1H1 siRNAs (B; see also corresponding Video 3, S9 and S10). Two-tailed Student's *t* tests show that the extent of spindle oscillations upon overexpression of $G\alpha i_1$-YFP or of YFP-LGN alone (Fig. 2, B and C) is statistically different from those in $G\alpha i_1$-YFP and DYNC1H1 siRNA (A) as well as in YFP-LGN and DYNC1H1 siRNA (B); in both cases, $P < 0.0001$. In contrast, the values in $G\alpha i_1$-YFP and DYNC1H1 siRNA (A), as well as in YFP-LGN and DYNC1H1 siRNA (B), are not statistically different from those in the control condition (Fig. 2 A); $P = 0.26$ and $P = 0.38$, respectively. Time is indicated in hours and minutes. The position of chromosomes is indicated by a white line. Error bars show SEM.

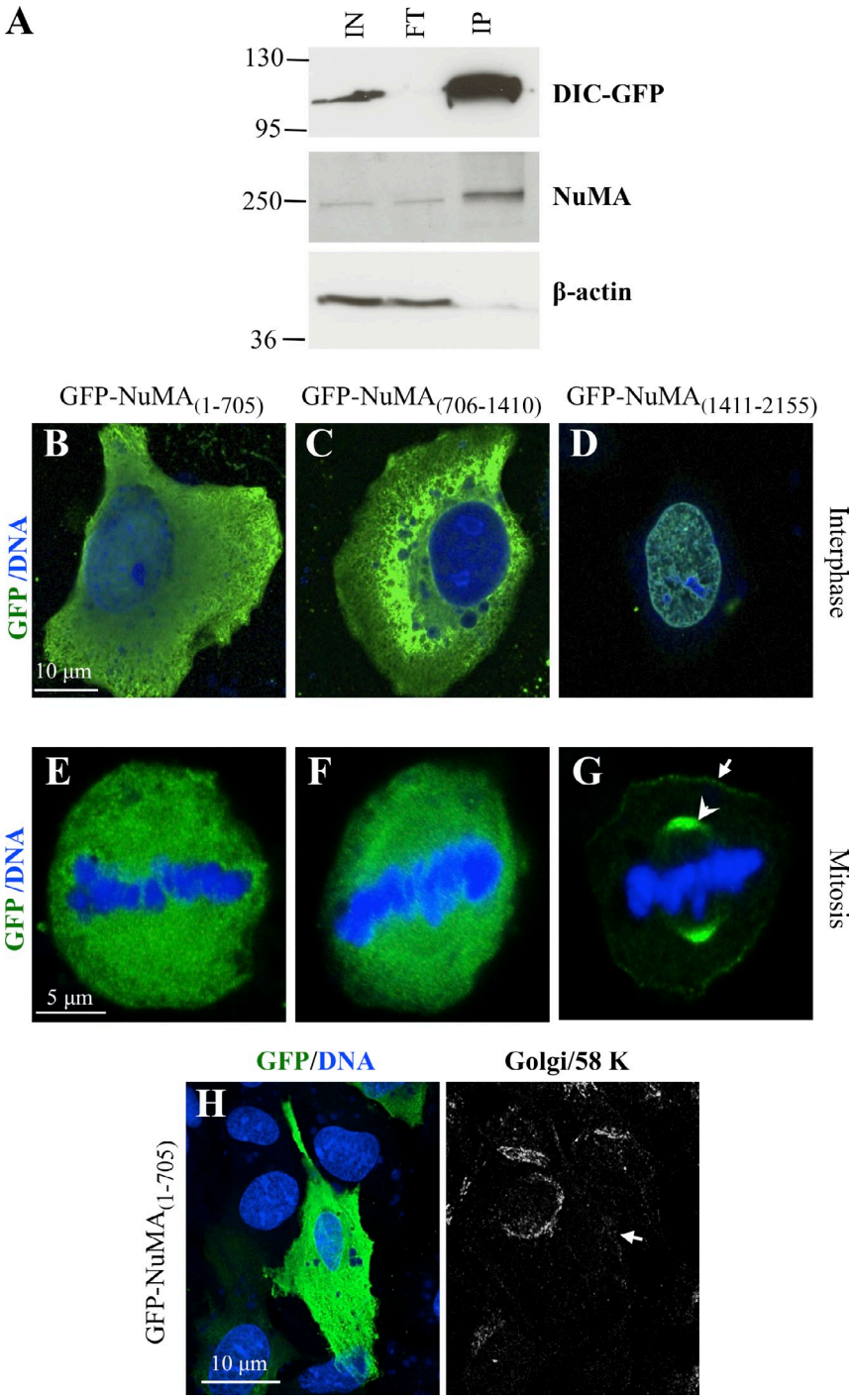

Figure S3. **NuMA interacts with dynein through its N-terminal part.** (A) Extracts from cells expressing multifunctional GFP-IC74 were immunoprecipitated with Ni–nitriloacetic acid beads, and the resulting blots were probed for GFP, NuMA, and β-actin, as indicated. Molecular mass is indicated in kilodaltons. IN, input (2.5% of total); FT, flow through (2.5%); IP, immunoprecipitate (10%). (B–G) HeLa cells in interphase (B–D) or mitosis (E–G) transfected with GFP-NuMA(1–705) (B and E) GFP-NuMA(706–1,410) (C and F), or GFP-NuMA(1,411–2,115) (D and G) and stained for GFP. Note that during interphase GFP-NuMA(1–705) and GFP-NuMA(706–1,410) both localize to the cytoplasm, whereas GFP-NuMA(1,411–2,115) localizes to the nucleus. During mitosis, GFP-NuMA(1–705) and GFP-NuMA(706–1,410) both localize to the cytoplasm, whereas GFP-NuMA(1,411–2,115) localizes to the spindle pole (arrowhead) and the plasma membrane (arrow). Over 100 cells were analyzed in each condition. (H) RPE-1 cells transfected with GFP-NuMA(1–705) stained for GFP and the 58K Golgi marker. Arrow points to a cell expressing GFP-NuMA(1–705), which exhibits Golgi dispersal. 50 cells were analyzed.

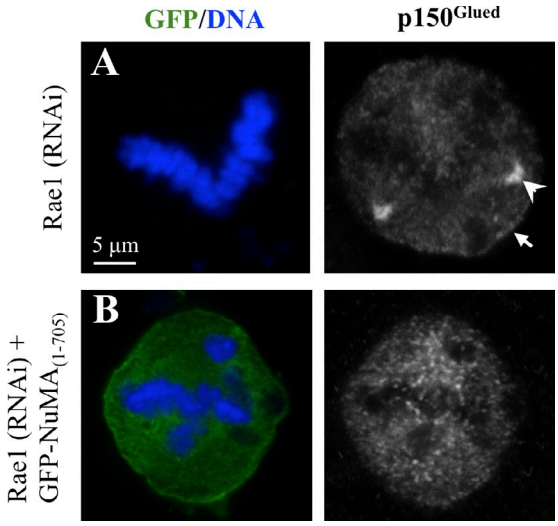

Figure S4. **NuMA(1–705) interferes with dynein function independently of Rae1.** (A and B) HeLa cells transfected with Rae1 siRNAs alone (A) or Rae1 siRNAi and GFP-NuMA(1–705) (B), fixed 60 h thereafter, and stained for GFP (left) and $p150^{Glued}$ (right). 50 cells were scored for each condition. Note that a third spindle pole in (A) is not visible in this particular focal plane. As reported previously (Wong et al., 2006), Rae1 depletion led to an increase in multipolar spindles (22% of cells vs. 2% of cells in control conditions; over 200 cells were scored in each condition). The arrow points to cortical $p150^{Glued}$, and the arrowhead points to the spindle pole pool of $p150^{Glued}$.

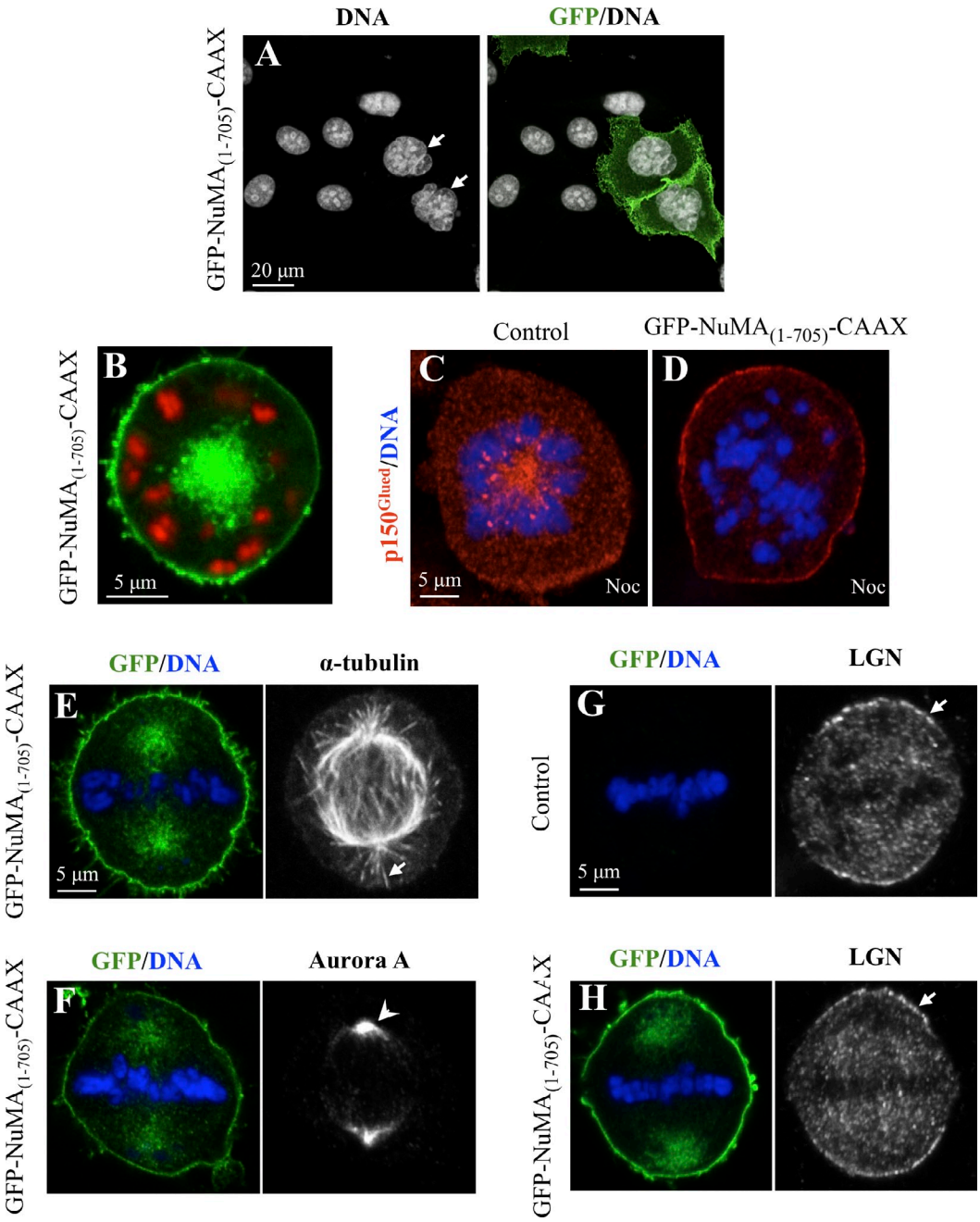

Figure S5. **Targeting the dynein-interacting part of NuMA to the plasma membrane results in mitotic phenotypes characteristic of dynein inhibition.** (A) Cells transfected with GFP-NuMA(1–705)-CAAX stained with a DNA dye and imaged also for GFP fluorescence. Arrows point to two binucleated/polyploid cells transfected with GFP-NuMA(1–705)-CAAX. Among two hundred cells, 13% exhibited binucleated/polyploidy upon transfection with GFP-NuMA(1–705)-CAAX compared with 2.5% in untransfected control conditions. (B) HeLa Kyoto mitotic cell stably expressing GFP–α-tubulin and mCherry-H2B as well as high levels of GFP-NuMA(1–705)-CAAX. Note the dispersed chromosomes. (C and D) Untransfected control HeLa cell (C) or cell transfected with GFP-NuMA(1–705)-CAAX (D) blocked in prometaphase for 18 h with 100 nM nocodazole (Noc) and stained for the dynactin subunit $p150^{Glued}$. Note loss of $p150^{Glued}$ from kinetochores in cells transfected with GFP-NuMA(1–705)-CAAX. (E and F) Cells transfected with GFP-NuMA(1–705)-CAAX and stained for α-tubulin (E) or Aurora A (F; each shown alone on the right) as well as GFP. Arrow in E points to astral microtubules; arrowhead in F points to the spindle pole. 55 cells were scored for each condition. (G and H) Untransfected control HeLa cell (G) or cell transfected with GFP-NuMA(1–705)-CAAX (H) stained for LGN (shown alone on the right) as well as GFP. Arrows point to cortical LGN. Note that LGN distribution is analogous in the two conditions. 25 cells were scored for each condition.

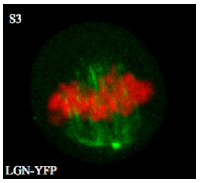

Video 1. **HeLa Kyoto cell stably expressing GFP–α-tubulin as well as mCherry-H2B and transfected with YFP, Gαi$_1$-YFP, or YFP-LGN.** S1 shows YFP; S2 shows Gαi$_1$-YFP; S3 shows YFP-LGN. S4 shows YFP-LGN expression in HeLa Kyoto cell expressing mCherry-H2B only; beside LGN localization at the cortex, note also distribution at spindle poles. Time-lapse videos were acquired using a laser-scanning confocal microscope (LSM 700) at one frame every 3 min and are played at 3 frames/s. Note severe oscillations in S2–S4 in comparison with S1.

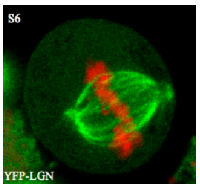

Video 2. **HeLa Kyoto cell stably expressing GFP–α-tubulin as well as mCherry-H2B and transfected with YFP or YFP-LGN.** S5 shows YFP; S6 shows YFP-LGN. Time-lapse videos were acquired using a laser-scanning confocal microscope (LSM 700) at one frame every 6 s and played at 3 frames/s.

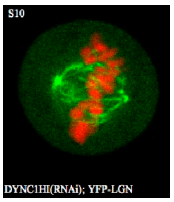

Video 3. **HeLa Kyoto cell stably expressing GFP–α-tubulin as well as mCherry-H2B and transfected with Gαi$_1$-YFP plus p150^{Glued} siRNAs, YFP-LGN plus p150^{Glued} siRNAs, Gαi$_1$-YFP plus DYNC1H1 siRNAs, or YFP-LGN and DYNC1H1 siRNAs.** S7 shows Gαi$_1$-YFP plus p150^{Glued} siRNAs; S8 shows YFP-LGN plus p150^{Glued} siRNAs; S9 shows Gαi$_1$-YFP plus DYNC1H1 siRNAs; S10 shows YFP-LGN and DYNC1H1 siRNAs. Time-lapse videos were acquired using a laser-scanning confocal microscope (LSM 700) at one frame every 3 min and played at 3 frames/s.

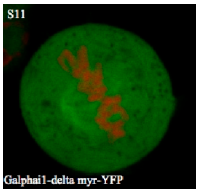

Video 4. **HeLa Kyoto cell stably expressing GFP–α-tubulin as well as mCherry-H2B and transfected with Gαi$_1$-Δmyr-YFP.** Time-lapse videos were acquired using a laser-scanning confocal microscope (LSM 700) at one frame every 3 min and played at 3 frames/s.

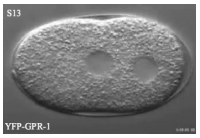

Video 5. **Time-lapse DIC microscopy of wild-type, YFP–GPR-1, or YFP–GPR-1 *dhc-1(RNAi)* one-cell stage *C. elegans* embryos.** S12 shows wild type; S13 shows YFP–GPR-1; S14 shows YFP–GPR-1 *dhc-1(RNAi)*. Anterior is on the left, and embryos are ∼50 µM long. Time-lapse videos were acquired using differential interference contrast microscopy (Axioskop 2 Plus; Carl Zeiss) at one frame every 5 s and played at 10 frames/s. Note excess spindle oscillations in S13 only.

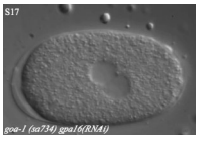

Video 6. **Time-lapse DIC microscopy of wild-type, *goa-1(n1134) gpa-16(RNAi)*, or *goa-1(sa734) gpa-16(RNAi)* one-cell stage *C. elegans* embryos.** S15 shows wild type; S16 shows *goa-1(n1134) gpa-16(RNAi)*; S17 shows *goa-1(sa734) gpa-16(RNAi)*. Anterior is on the left, and embryos are ∼50 µM long. Time-lapse videos were acquired using differential interference contrast microscopy (Axioskop 2 Plus) at one frame every 5 s and played at 10 frames/s. Note loss of spindle oscillations and equal division of embryo in S16 and S17.

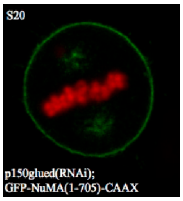

Video 7. **HeLa Kyoto cell stably expressing GFP–α-tubulin as well as mCherry-H2B and transfected with GFP-NuMA(1–705)-CAAX, GFP-NuMA(1–705), or transfected with GFP-NuMA(1–705)-CAAX plus p150^{Glued} siRNAs.** S18 shows GFP-NuMA(1–705)-CAAX; S19 shows GFP-NuMA(1–705); S20 shows GFP-NuMA(1–705)-CAAX plus p150^{Glued}. Time-lapse videos were acquired using laser-scanning confocal microscope (LSM 700) at one frame every 3 min and played at 3 frames/s. Note severe spindle oscillations upon overexpression of GFP-NuMA(1–705)-CAAX (S18); note also loss of oscillations upon depletion of p150^{Glued} in cells expressing GFP-NuMA(1–705)-CAAX (S20).

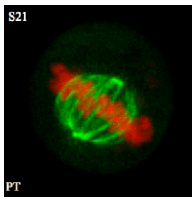

Video 8. **HeLa Kyoto cell stably expressing GFP–α-tubulin as well as mCherry-H2B HeLa Kyoto cells treated with pertussis toxin or transfected with GFP-NuMA(1–705)-CAAX plus treated with pertussis toxin.** S21 shows a pertussis toxin–treated cell; S22 shows GFP-NuMA(1–705)-CAAX plus pertussis toxin. Time-lapse videos were acquired using a laser-scanning confocal microscope (LSM 700) at one frame every 3 min and played at 3 frames/s. Note that treatment with pertussis toxin (PT) does not impair spindle oscillations upon GFP-NuMA(1–705)-CAAX expression (S22).

Reference

Wong, R.W., G. Blobel, and E. Coutavas. 2006. Rae1 interaction with NuMA is required for bipolar spindle formation. *Proc. Natl. Acad. Sci. USA*. 103:19783–19787. http://dx.doi.org/10.1073/pnas.0609582104